

DETERMINATION OF TRACE ELEMENTS IN ICE CORE SAMPLES BY LASERABLATION INDUCTIVELY COUPLED PLASMA MASS SPECTROMETRY

H. Reinhardt, M. Kriews, O. Schrems, C. Lüdke¹, E. Hoffmann¹ and J. Skole¹

Alfred Wegener Institute for Polar and Marine Research, Am Handelshafen 12,
D-27570 Bremerhaven

¹Institute for Spectrochemistry and Applied Spectroscopy, Albert-Einstein-Straße 9,
D-12489 Berlin

1 INTRODUCTION

The snow and iceshields of the polar regions serve as a climate archive and deliver a useful insight back to about 250.000 years of earth climate history^{1,2}. The aim of our investigation reported here was to establish a new method for the determination of trace elements in ice cores from polar regions with Laserablation Inductively Coupled Plasma Mass Spectrometry (LA-ICP-MS)³. Primarily, the construction of a cryogenic laserablation chamber and the optimization of the analysis system for the sample matrix were the main goals. This paper reports preliminary results from measurements of frozen ice samples, the achievable signal intensities, standard deviations and calibration graphs as well as the first signal progression of ²⁰⁸Pb in an 8000 years old ice core sample from Greenland.

1.1 The Advantages Of The New LA-ICP-MS Application

LA-ICP-MS offers the possibility of direct analysis of deep frozen ice core samples from the polar regions. The main advantages are:

- low risk of contamination in contrast to conventional solution ICP-MS
- a high spatial and time resolution from 200 to 1000 µm (recording of depth profile) dependent on the spotsize of the laser crater

With such a high spatial resolution it will be possible to detect seasonal variations of the element distribution and composition also in deep ice layers where annual layers have a thickness of only about 1 mm. Up to now, element analytical determinations of ice core samples were only possible with molten ice samples. After a special sample preparation including enrichment procedures and addition of chemicals, the samples were analysed with chemical-physical methods^{4,5}. As concentrations in such samples are very low (ppt-level), the risk of contamination during sample preparation is very high. Due to the need of relative high volumina in solution analysis, only a small spatial (cm-level) and therefore a reduced temporal resolution of molten ice core samples is possible.

1.2 Tracer Elements In Ice Cores

The distribution and composition of trace elements in annual layers of ice cores can for example provide information about the changes from cold to warm periods (e.g., increase of mineral dust or seasalt), special events in earth history like volcanic eruptions (dust horizons in ice core layers) or pointing to sources for mineral dusts^{6,7,8}. The detection of seasonal variations of mineral dust and seasalt concentrations can give valuable hints for the dating of the ice cores.

1.2.1. Elements Of Interest. Sodium and magnesium are tracer elements for seasalt, aluminum and iron are mineral dust tracers. The seasalt and the mineral dust concentrations in arctic snow and ice samples vary with the season. Due to the progression of the polar front in summer and winter time, airmasses bring more or less seasalt or mineral dust into the Arctic which are deposited on snow and ice. Lead, zinc and cadmium are tracers for anthropogenic sources or indicators of contamination effects. The concentrations of these elements can also show seasonal variations.

2 EXPERIMENTAL SECTION

2.1 Experimental Setup

Figure 1 illustrates the experimental setup for the direct analysis of deep frozen ice samples by Laserablation ICP-MS.

2.1.1. Laser System. For many applications the use of UV wavelengths (e.g. 266 nm) for laserablation is more suitable because UV radiation can be focused to a smaller spot than longer wavelengths radiation and because it is stronger absorbed by many materials than visible and IR laser radiation⁹. Whereas the absorption coefficient of ice at UV wavelengths is about two orders of magnitude lower than at 1064 nm¹⁰, i.e. ice is more translucent and less material would be ablated. Based on that the laser used was a modified Nd:YAG (DCR-11, SPECTRA PHYSICS) operated at 1064 nm. A power measurement unit and an aperture system are installed behind the beam exit to control laser energy and spotsize.

2.1.2. Sample Alignment. For an exact alignment of the sample inside the laserablation chamber, an diod laser (red) is integrated on the optical axis of the Nd:YAG laser beam. With support of a CCD color camera the laser beam is focussed on the sample surface and the ablation process can be viewed.

2.1.3. Laserablation Chamber. To enable a direct analysis of solid ice samples at a temperature of -30°C a special laserablation chamber was constructed¹¹. -30°C is the standard temperature for the storage of ice core samples because no changes inside the ice takes place at these low temperatures. The chamber has a large volume to enable the measurement of ice core samples cut as discs (diameter: 10 cm) or segments with one or more annual layers depending on the depth of the ice origin. The inner part of the chamber consists of high purity copper and contains a cooling canal for the cooling liquid (silicon oil). The outer shell consists of teflon and enables a good insulation against the copper block. The carrier gas (argon) is cooled to avoid droplets of water at the optical window and to prevent melting processes at the sample surface during the ablation process. A computer controls the sample stage of the laserablation chamber in xyz-orientation as well as the laser system.

2.1.4. ICP-MS System. The measurements were carried out using the quadrupole based ICP-MS System ELAN 6000 from PERKIN ELMER/SCIEX. An

argon flow rate of 1.2 l min^{-1} carries the ablated material into the plasma (tube length = 100 cm), for ionization and subsequent analysis in the mass spectrometer.

2.2 Operating Conditions

Tables 1 and 2 give an overview over the optimized operation parameters used with the ICP-MS system and the Nd:YAG laser.

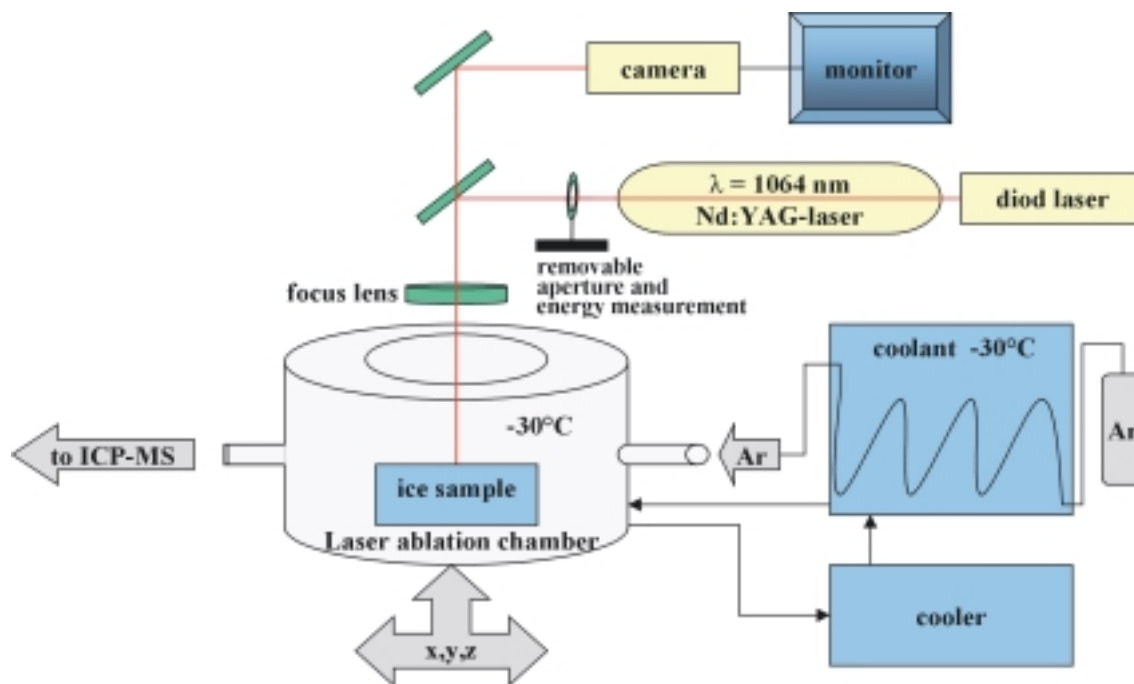


Figure 1 Experimental setup for the laser ablation of solid ice samples

Table 1 Operating conditions for the ICP-MS system

ICP mass spectrometer	Perkin Elmer Sciex Elan 6000
RF Power	1400 W
plasma gas	15 L min^{-1}
auxiliary gas	0.8 L min^{-1}
carrier gas	1.2 L min^{-1}
lens setting	autolens mode on
measuring mode	peak-hopping
isotopes measured	^{17}OH , ^{19}OH , ^{23}Na , ^{24}Mg , ^{27}Al , ^{44}Ca , ^{64}Zn , ^{103}Rh , ^{114}Cd , ^{208}Pb
dwel time	20 ms
detector mode	dual (pulse and analogue)

Table 2 Operating conditions for the Laser system

laser sampler	Perkin-Elmer Laser Sampler 320
wavelength	1064 nm
mode	Q-switch
Q-switch time	220 μ s
excitation lamp energy	50 J
laser energy	300 mJ
pulse frequency	10 Hz
laser scan mode	point, line
focus	on sample surface

2.3 Preparation of Ice Standards

A major problem of LA-ICP-MS as a method for quantitative determination, is the calibration with matrix matched standards. Therefore it seems to be an easy task to make a calibration with frozen standard solutions for the quantitative determination in ice samples. Due to the expected values of trace elements in ice core samples from the Arctic^{1,2}, low concentration standards of some elements were prepared. We found a procedure for the preparation of suitable ice standards with different element concentrations (10 ng/L to 100 μ g/L). Commercial available ICP-MS multielement solutions (PE 1 and PE 2: PERKIN ELMER company) were filled up in pre-cooled purified petri dishes (diameter: 5 cm, height: 1 cm) after dilution and addition of nitric acid at a temperature of -30°C in our ice laboratory. All preparation steps were performed under cleanroom conditions (US-class 100). The petri dishes and the sample carrier run through a special cleaning procedure with different acid bassins before using. To prevent inhomogenities in ice standards the fill up was made step by step to a maximum height of 1 cm. In 5 ml steps the standard solutions were given into the petri dishes to enable a shock freezing of the solution. It seems, that, on one hand, an enlarged thickness leads to inhomogenously frozen samples, whereas a thinner layer is pervious for the laser beam, and the surface of the sample carrier will be hit. Furthermore it seems, that a higher concentrated solution (over 100 μ g/L) leads to strong inhomogenously frozen ice and delivers more unstable signals. The ice standards are stored under a clean bench at -30°C .

2.4 Ice Sample Preparation

2.4.1. Different Sample Shapes. There are two possible ways to cut an ice core sample for trace element determination with LA-ICP-MS: Ice core discs and segments (Figure 2). The cutting of the cores is carried out in an ice laboratory at -30°C under clean room conditions. A ceramic working bench with ceramic knives or knives made of high purity molybdenum were used. The samples were frozen on object slides and have a maximum thickness of 1 cm. To enable focussing of the laser beam during the measurement, a plane sample surface is required. The discs have a diameter of 10 cm, the segments a length of 10 and a width of 5 cm.

2.4.2. Ablation Patterns. The ice core disc is more suitable for contamination studies. To have a look on contaminations coming from the ice core driller², the point scan mode was chosen (laser spots move from wall towards the center). At the point scan mode, the laser shot a certain time at the same point on the surface of the ice sample. The other possible shape is the ice core segment which is more suitable to record depth profiles. The age and therefore the depth of the ice has a horizontal

direction instead of vertical direction at a disc. The point scan mode was used as well as the line scan where the laser shot along a defined line.

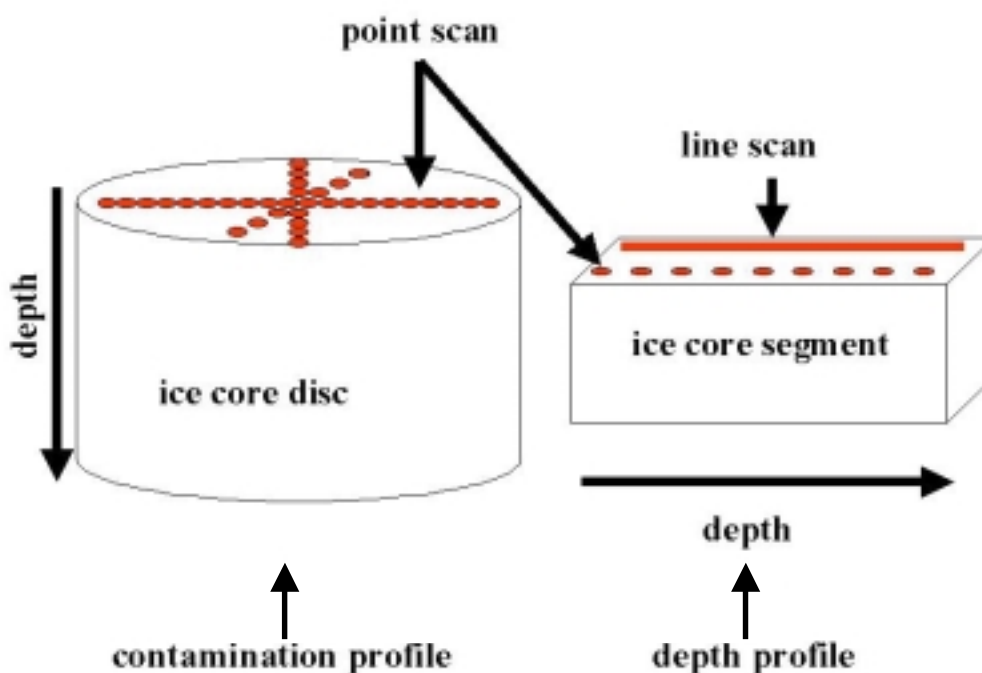


Figure 2 Different ablation pattern along an ice core disc and an ice core segment

3 RESULTS

3.1 Signal Progression

In figure 3 the progression of a ^{103}Rh and a ^{208}Pb signal from a line scan of a $100\ \mu\text{g/L}$ ice standard are plotted. The arrow indicates where the laser started to fire. After a short forerun of about 30 seconds the signal becomes stable. A defined line on the sample surface is scanned several times. The focus of the laser beam is orientated on the sample surface. The removal of ablated material from the ice surface is approximately $30\ \mu\text{g}$ per lasershot. For ^{103}Rh we could reach a maximum signal intensity of about 400.000 counts per second, for ^{208}Pb 600.000 counts per second under optimized conditions (see table 1 and 2). It is demonstrated, that the measurement of frozen ice standards leads to a linear signal dependence as known from the work with solutions. Due to the relative large dimension of the laserablation chamber, the wash out time is about 7 minutes dependent on the standard concentration.

3.2 Calibration Studies

In figure 4 the ^{208}Pb signal progression of ice standards at different concentrations is demonstrated. The measurement time is 150 seconds what is shown to be an adequate time where the laser signal ist most stable. A $10\ \text{ng/L}$ (ppt) ice standard signal can be distinguished very well between the signal of a blank.

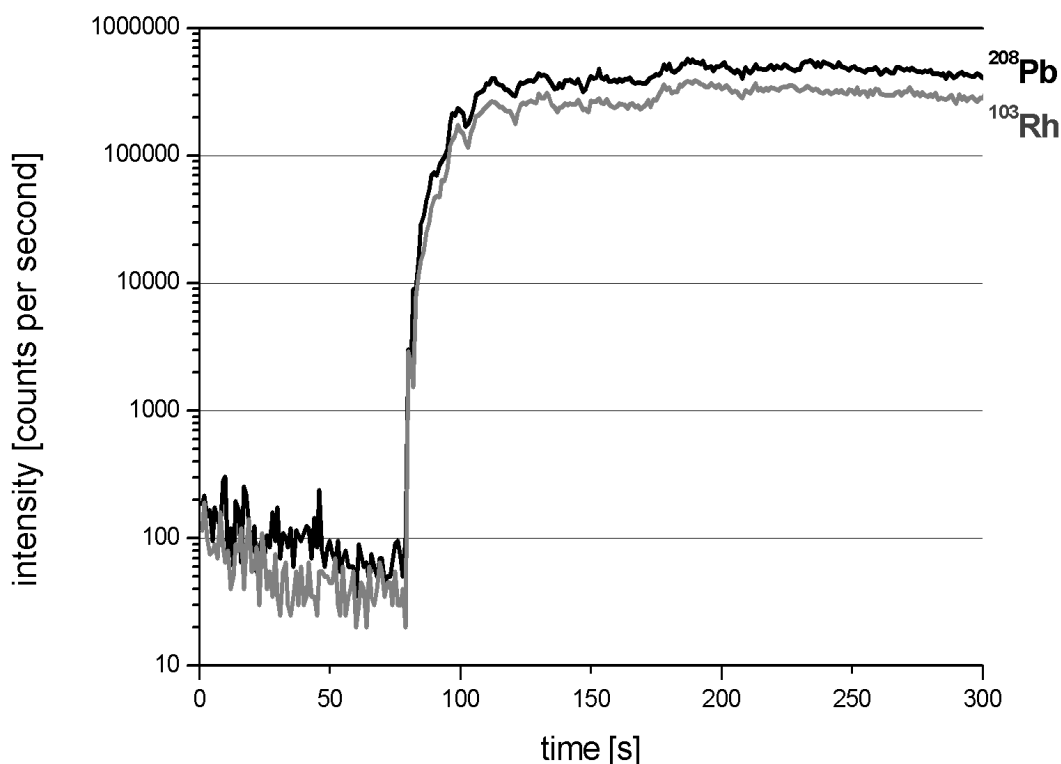


Figure 3 Signal progression of a 100 µg/L ice standard

3.2.1. Calibration graphs. The element lead could be calibrated very well with 5 standards from 10 ng/L up to 100 µg/L plus the blank (n = 6). The resulting regression coefficient was $R = 0.99966$, the measured time $t = 150$ s. Table 3 lists the resulting coefficients of correlation (R), where n is the number of used ice standards for the calibration curve, $n < 6$ indicates that lower standards were not used for calibration. An example for an element which is difficult to calibrate is calcium. Here, the lower concentrated ice standards resulted in very instable signals and no good linear dependence was obtained. The relative high signals of ^{44}Ca in the blank and the low concentrated standards inhibit a calibration in the ng/L level (n = 3; 1, 10 and 100 µg/L). Altogether, calibration graphs of 7 isotopes were performed: ^{23}Na , ^{24}Mg , ^{27}Al , ^{44}Ca , ^{64}Zn , ^{114}Cd , ^{208}Pb .

Table 3 Coefficients of correlation (R) for the calibration graphs

internal standard	^{23}Na	n	^{24}Mg	n	^{27}Al	n	^{44}Ca	n	^{64}Zn	n	^{114}Cd	n	^{208}Pb	n
none	0.9987	4	0.9995	6	0.9991	4	0.9999	3	0.9996	6	0.9993	4	0.9999	6
^{17}OH	0.9985	4	0.9993	6	0.9914	4	1	2	0.9997	4	0.9991	4	0.9997	6

3.2.2. *Internal Standard.* As known from solution ICP-MS, the use of an internal standard like rhodium is important to reduce the influence of signal variations coming from the drift of the ICP-MS. In real ice samples there is not a possibility to spike the sample. The main reasons for the relative high signal variations are inhomogeneities of the ice standards and a different removal of material from the ice surface due to unevenness or fluctuations in laser energy. Table 4 shows the relative standard deviations in percent obtained with no internal standard as well as ^{17}OH and ^{19}OH as internal standards. The measuring time of the 10 ppb standard was 60 seconds. The ^{17}OH and ^{19}OH signals originated from the water of the ice sample and depend on the removal of material during the ablation process. With the use of ^{17}OH as internal standard an improvement of about 3 to 5 percent of RSD could be achieved. The RSDs shown in table 4 are higher than the achieved values in figure 5. The values in figure 5 were obtained with more homogeneous ice standards (preparation is shown in part 2.3.).

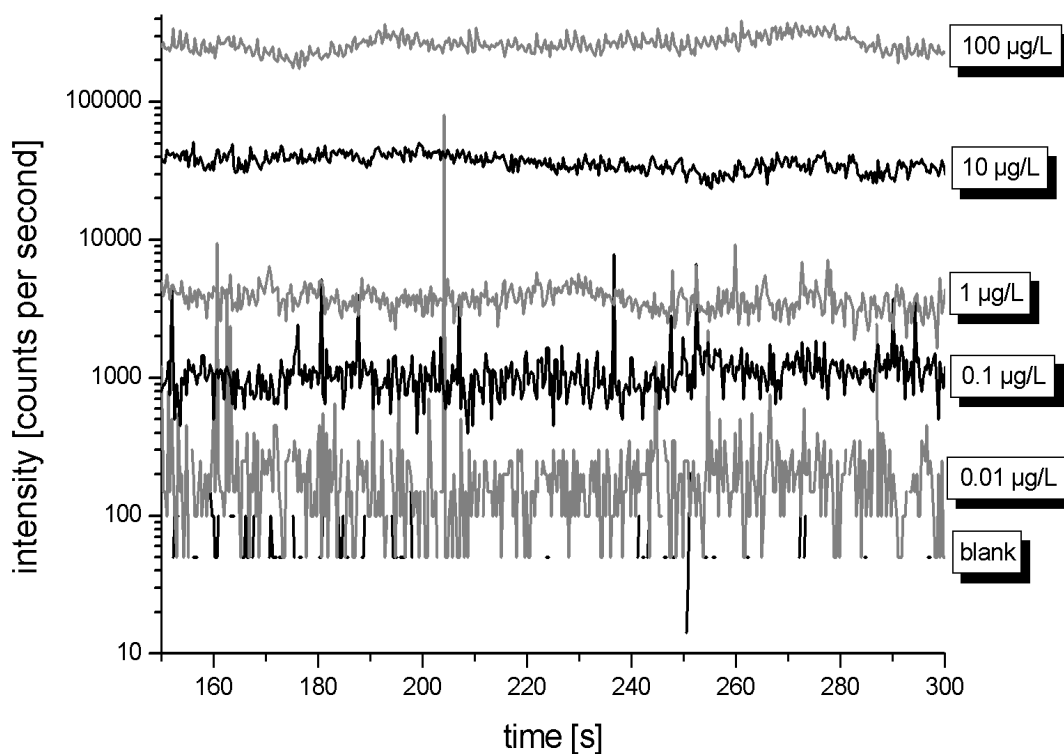


Figure 4 ^{208}Pb signal progression of different ice standards

Table 4 Relative standard deviations (%) with and without internal standard

internal standard	^{23}Na	^{24}Mg	^{27}Al	^{44}Ca	^{64}Zn	^{114}Cd	^{208}Pb
none	17	17	16	9	17	17	17
^{17}OH	14	14	14	3	15	15	14
^{19}OH	15	14	14	5	15	15	15

3.3 Daily Performance Ice Standard

It is useful to prepare a frozen daily performance standard with a selected content of elements (Be, Mg, Co, Ni, In, Ce, Pb, Bi, U) to check the performance of the measurement devices. Figure 5 illustrates the reachable intensities, relative standard deviations and the formation ratio of oxides and doubled charged ions of a 10 µg/L daily performance ice standard. The RSDs are in the range of about 3 to 6 percent (bars). The number of repetition measurements was 6. The black boxes indicate the reached intensities of the elements. Due to the fact of an relative dry laser aerosol the oxide rate was less than 0.2 per cent, the double charged ions were below 1 per cent.

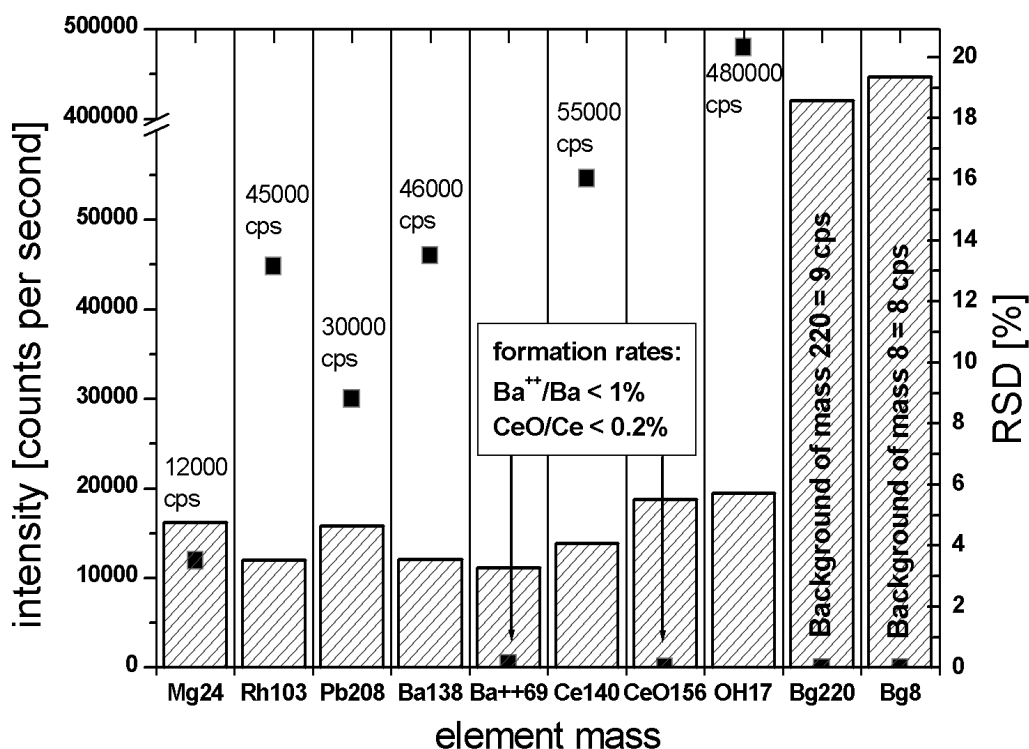


Figure 5 Signal intensities and RSDs of a 10 µg/L daily performance ice standard

3.4 Background Noise

Generally, aerosols which are produced by laser ablation are dry and lead to an increased background noise at the mass 220. During laser ablation of ice samples, argon which is used as carrier gas seems to take up water vapour from the probe. A comparison of different sample introduction systems shows a background of 10 – 40 cps for the laser and hence, the values are below the ones produced by a microconcentric nebulizer (60-100 cps); MCN 6000, CETAC company. On the other hand, results obtained from a cross flow nebulizer are drastically lower (1-3 cps). Therefore, the relatively low background noise caused by the laser aerosol shows a positive effect on the detection limits. According to the alignment of the microconcentric nebulizer a plasma power of 1400 W has been chosen for the laser aerosol.

3.5 ^{208}Pb Signal Progression Of A Real Sample

Figure 6 shows a signal progression of an analysed real sample (ice core segment). The sample is from Greenland from a depth of 1100 m and is about 8000 years old. After 40 seconds of forerun the laser begun to fire along a defined line. At the end of the sample (6 cm), the laser turns and goes back along the same line. The solid line shows the smoothed signal progression of lead. Similar signatures were obtained for the move fore and backwards the line scan of the laser. A calculation into concentrations with the help of the calibration graph for lead results in 10 to 20 ng/L for the sample. This value is in a good agreement with data from Boutron¹ for the GRIP core in this depth.

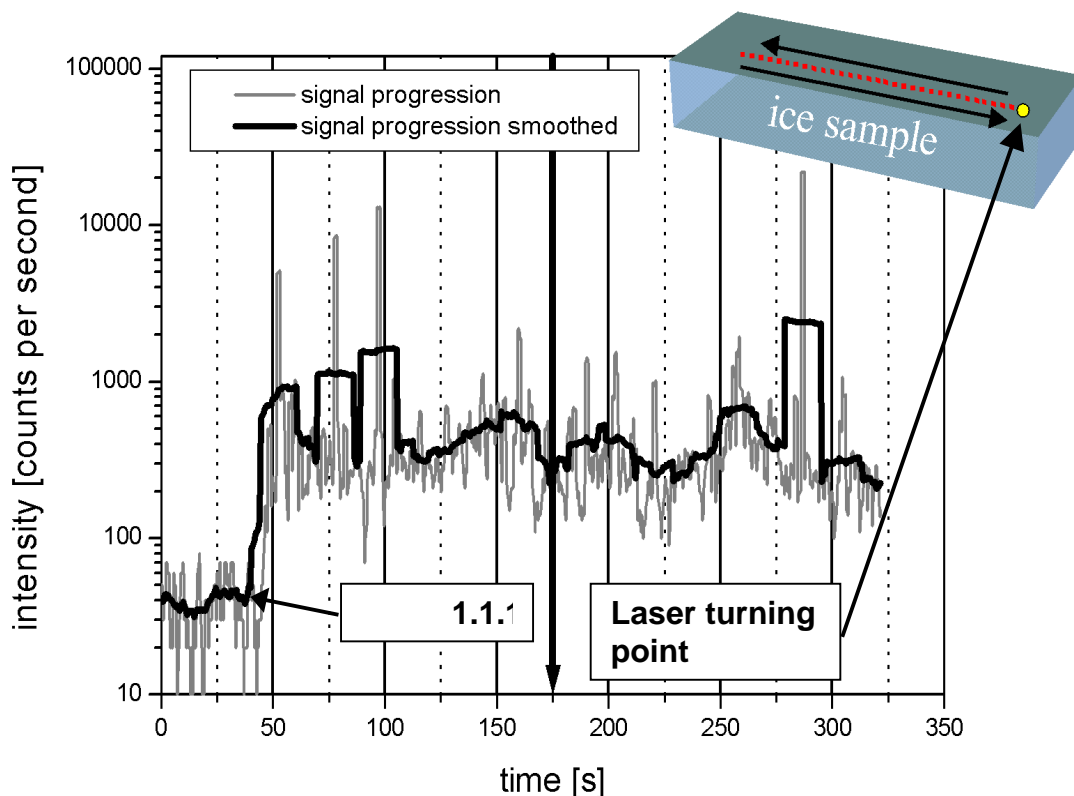


Figure 6 ^{208}Pb signal progression of a real ice sample (Greenland)

4 DISCUSSION AND OUTLOOK

Preliminary results for direct measurements of frozen ice samples by LA-ICP-MS have shown high counting rates and stable signals. The data gave promising indications that element signatures in polar ice cores could be obtained. In comparison to solution analysis with a Cross Flow Nebulizer the counting rates are lower by the factor of 3, however the measurement occurs directly from the solid. In spite of a special sample preparation the freezing process of the standard solution is the main cause for inhomogenities inside the ice sample and leads therefore to variations of the analyt signal. In the future we will try to prepare more homogeneous ice standards by shock-freezing at -195°C with liquid nitrogen. Examinations with a cryo-electron microscope will be carried out to check if shock-frozen ice standards are amorphous and therefore more homogeneous.

5 REFERENCES

1. C. F. Boutron, S. Hong, J.P. Candelone, *Proceedings of the International Conference: Heavy Metals in the Environment*, University of Hamburg, 1995, **1**, 28.
2. M. Legrand, R. Delmas, in *European Research Course on Atmospheres: Topics in Atmospheric and Interstellar Physics and Chemistry*, Grenoble, 1994, Chapter 19, p. 387.
3. M. Kriews, H. Reinhardt, E. Hoffmann, C. Lüdke, Declaration of Invention AWI 01/0799 DE, file number DE 199 34 561.9-52, Deutsches Patent- und Markenamt, München, 1999.
4. M. Kriews, I. Stölting, J. Kipfstuhl, O. Schrems, *Proceedings of the 14. ICP-MS User Meeting*, University of Mainz, 1998, P10.
5. S. Matoba, M. Nishikawa, O. Watanabe, Y. Fujii, *J. Environ. Chem.*, 1998, **8**, 421.
6. J. M. Palais, S. Kirchner, R.J. Delmas, *Annals of Glaciology*, 1990, **14**, 216.
7. G. A. Zielinski, P. A. Mayewski, L. D. Meeker, K. Grönvold, M. S. Twickler, K. Taylor, *J. Geophys. Res.*, 1997, **102**, 26625.
8. G. A. Zielinski, M. S. Germani, *J. Archaeolog. Science*, 1998, **25**, 279.
9. D. Günther, S. E. Jackson, H. P. Longerich, *Spectrochimica Acta Part B*, 1999, **54**, 381.
10. S.G. Warren, *Applied Optics*, 1984, **23**, No. 8, 1206.
11. M. Kriews, H. Reinhardt, I. Beninga, E. Dunker, Declaration of Invention AWI V/99 KRBD, Deutsches Patent- und Markenamt, München, 1999.